doi: 10.4149/gpb_2024045

GZMA silencing inhibits JAK2/STAT1 pathway and improves allergic rhinitis

Lin Li[1], Yuhao Zhang[1], Jingyuan Wang[1], Lixia Zhang[1], Ying Gao[1], Xiaolin Ji[1], Tian Wang[1] and Fei Zhao[1]

[1] *Department of Otolaryngology Head and Neck Surgery, Shanxi Bethune Hospital, Shanxi Academy of Medical Sciences, Third Hospital of Shanxi Medical University, Tongji Shanxi Hospital, Taiyuan, Shanxi, China*

Abstract. Allergic rhinitis (AR) is an immunoglobulin E (IgE)-mediated inflammatory disorder. This study attempts to identify AR-related differential expressed genes (DEGs) and determine potential targets for AR. We employed bioinformatics analysis to screen for hub DEGs for AR, and their performances in distinguishing AR were assessed by receiver operating characteristic (ROC) curves. Quantitative reverse-transcription polymerase chain reaction (qRT-PCR) and Western blot was used to quantify Granzyme A (GZMA) in ovalbumin (OVA)-induced AR mice. TNF-α-induced cell model was utilized to assess the role of GZMA in AR, and the effect of GZMA silencing on the JAK2/STAT1 pathway was investigated in TNF-α-induced AR. We identified HIST1H2BD, RPS28, HIST1H1C, MAF, and GZMA as hub genes, all of which exhibited excellent performance in distinguishing between AR and controls (AUC > 0.800). GZMA was highly expressed in AR mice. Silencing GZMA reduced the levels of inflammatory cytokines (IL-6, IL-4 and IL-5), inhibited cell apoptosis and promoted cell proliferation in TNF-α-induced nasal mucosal epithelial cells (MIC-iCell-m024). Overexpression of GZMA exhibited the opposite effects by promoting inflammation and cell apoptosis but inhibiting proliferation. Mechanistically, silencing GZMA inhibited the phosphorylation of JAK2 and STAT1, indicating the suppression of JAK2/STAT1 pathway. This study might share new idea for AR management.

Key words: Allergic rhinitis — JAK/STAT — GZMA — Inflammation response

Introduction

Allergic rhinitis (AR) is a global health disorder characterized by hypersensitivity reaction induced by the inhalation of allergenic particles and immunoglobulin E (IgE)-mediated inflammation, which brings significant medical and economic challenges (Nur Husna et al. 2022b). In China, the prevalence of AR stands at 19% among adults and 22% among children, with boys being more affected than girls (Pang et al. 2022). It has been reported that other allergic diseases such as asthma, allergy history and passive smoking, as well as air pollutants such as particulate matter, are major risk factors leading to the AR development (Lin et al. 2021; Pang et al. 2022). Recently, increasing evidence has revealed the role of crucial immune cells, including type 2 innate lymphocytes (ILC2s), T helper type 2 (Th2) cells, follicular helper T cells, follicular regulatory T cells, regulatory T cells, B cells, dendritic cells (DCs), and epithelial cells, in compromising the epithelial barrier. This impairment leads to the allergic reactions and favorable responses to therapeutics for AR (Zhang et al. 2022). Allergen-specific immunotherapy remains the sole method for desensitization, while other methods are still in the exploratory stage in AR (Zhang et al. 2022). Therefore, it is necessary to develop novel targets of AR treatment.

The Janus kinase/signal transducer and activator of transcription (JAK/STAT) pathway is important for homeostasis

Electronic supplementary material. The online version of this article (doi: 10.4149/gpb_2024045) contains Supplementary material.

Correspondence to: Fei Zhao, No. 99, Longcheng Street, Xiaodian District, Taiyuan City, Shanxi Province, 030032, China
E-mail: zhaofei3333@163.com

in human body through signal transduction (Qayum et al. 2020). This pathway participates in various cellular processes and involves in cancer, inflammatory, and immune diseases (Hu et al. 2021). In some allergic diseases, such as AR and asthma, compelling evidence has found that elevated STAT6 expression is associated with NK cell-mediated Th2 cytokine release, leading to allergic inflammation (Gotthardt et al. 2019). α-linolenic acid represses JAK/T-bet/STAT1 and JAK/GATA3/STAT6-mediated inflammatory responses in AR *via* restoring Th1/Th2 balance (Ren et al. 2022). The JAK/STAT pathway inhibitor CYT387 (momelotinib) attenuates AR by inhibiting JAK/STAT pathway to abolish DCs-mediated Th2 cell responses (Shi et al. 2017). Furthermore, Xiaoqing-long-tang, a traditional Chinese medicine compound, has been demonstrated to alleviate type 2 responses in AR by the regulation of interleukin-33 (IL-33)/ST2 and JAK/STAT-mediated innate lymphoid cells (Zhang et al. 2023). Although STAT1 has been implicated in the pathogenesis of Schistosoma mansoni egg antigen-caused AR (Hattori et al. 2007), the role of JAK2/STAT1 in AR remains unclarified.

The identification of differential expressed genes (DEGs) has been used as a useful tool to comprehensively study the underlying pathogenesis of diseases and to determine therapeutic biomarkers. In the present study, DEGs were identified between AR samples and non-allergic controls based on expression profiling data from the Gene-Expression Omnibus (GEO) database. Granzyme A (GZMA), one of the granzymes, belongs to the homologous serine proteases family. When target cells are attacked by cytotoxic lymphocytes, such as natural killer (NK) cells and cytotoxic T lymphocytes (CTLs or CD8+ T cells), GZMA is released and delivered into the target cell cytosol by perforin, leading to apoptotic cell death (Martinvalet et al. 2005). Besides, Zhou has found that NK cells and CTLs cleaves gasdermin B to induce the pro-inflammatory cell death pyroptosis (Zhou et al. 2020). It has been recognized that GZMA is a mediator of inflammation and involves in various inflammatory diseases (Schanoski et al. 2020). However, there are limited reports on the role of GZMA in AR.

Apoptosis is a form of programmed cell death caused by exposure to a specific condition, in order to eliminate harmful, damaged or unwanted cells. The balance between apoptosis and cell proliferation is necessary for various physiological processes (Voss et al. 2020). An imbalance between proliferation and elimination of the cells may contribute to the development of inflammatory responses (Grzegorczyk et al. 2002). It has been reported that the inhibition of apoptosis and increased proliferation of nasal mucosa cells is associated with alleviation of AR by regulating the JAK/STAT3 pathway (Huang et al. 2021). Hence, it is crucial to evaluate the level of cell proliferation and apoptosis in AR, in addition to the inflammatory response. In the present, we investigated the effects of GZMA silencing and overexpression on inflammatory responses, cell viability, proliferation and apoptosis in TNF-α-induced AR cell model. Additionally, we evaluated the inhibitory effect of GZMA silencing on JAK/STAT pathway.

Material and Methods

Data collection

Expression profiling data for patients with seasonal AR was downloaded from GSE18574 and GSE43523 datasets in the GEO (https://www.ncbi.nlm.nih.gov/geo/) database by retrieving "Allergic rhinitis". In the GSE18574 dataset, samples were collected from 3 patients with seasonal AR; each sample was separated into allergen-challenged and unchallenged control groups. In the GSE43523 dataset, nasal epithelial cells were obtained from 7 seasonal AR patients and 5 non-allergic controls. Prior to analysis, data was normalized and the overview of data distribution was displayed using boxplots.

Screening of DEGs

GEO2R (https://www.ncbi.nlm.nih.gov/geo/geo2r/) was used to screen for genes that were differentially expressed between AR samples and non-allergic controls within GSE18574 and GSE43523 datasets. DEGs were identified under the criteria of $p < 0.05$ and $|\log2\text{FoldChange}| \geq 0.5$ (AR *vs.* Control). Next, upregulated and downregulated DEGs were visualized using volcano plots, while their expression patterns were displayed in a heatmap. A Venn diagram was drawn through EVenn (http://www.ehbio.com/test/venn/#/) to determine the common DEGs (co-DEGs) at the intersection of DEGs between GSE18574 and GSE43523 datasets. Based on the DEGs in these two datasets, gene set enrichment analysis (GSEA) (Subramanian et al. 2005) was performed to determine the significantly enriched biological pathways among the DEGs.

Functional enrichment analyses

We conducted Gene Ontology (GO) and Kyoto Encyclopedia of Genes and Genomes (KEGG) functional enrichment analysis for the co-DEGs using the bioinformatics platform (http://www.bioinformatics.com.cn/). The GO categories included biological process (BP), cellular component (CC) and molecular function (MF). Candidates with a p value < 0.05 were selected as significantly enriched pathways.

Generation of protein-protein interaction (PPI) network

To predict the interaction relationships between gene-coded proteins in AR, Search Tool for the Retrieval of Interacting Genes/Proteins (STRING) database (https://www.string-db.

org/) (Franceschini et al. 2012) was applied to generate a PPI network for co-DEGs with a confidence score > 0.400. Cytoscape (www.cytoscape.org/) (Kohl et al. 2011) was employed to visualize this PPI network. Subsequently, the tightly connected protein clusters were screened by molecular complex detection (MCODE) algorithm, and the degree of each protein node was calculated using CytoHubba plug-in (version 0.1).

Analysis of hub genes

Ridgeline plots were used to evaluate data distribution using "ggridges" R package (Wilke 2018). Additionally, we visualized the association matrices for hub genes using correlation heatmaps based on "corrplot" R package (Wei et al. 2017). p value < 0.05 was considered as significant correlation. In addition, principal components analysis (PCA) was conducted based on the expression of hub gene in GSE43523 dataset. To determine the diagnostic accuracy of hub genes in AR, receiver operating characteristic (ROC) curves, along with the area under the ROC curves (AUCs), were used. Briefly, these curves were plotted using pROC package in the Bioinformatics online database (http://www.bioinformatics.com.cn/) based on data from the GSE43523 dataset. When inputting the data, we organized the information with the sample names in the first column, the classification (with two categories) in the second column, and the gene expression values in the third and subsequent columns.

Induction of AR model

Experiments were performed according to the guidelines for laboratory animal care and approved by the Local Ethics Committee (Ethics Number: 2022GLL127).

To address hormonal changes and estrous cycles, as well as to ensure standardization and consistency, male BALB/c mice were employed for this study (Ri et al. 2019; Dong et al. 2020). SPF male BALB/c mice (6–8 weeks, 20–22 g) were purchased from SPF Biotechnology Co., Ltd. (Beijing, China) and housed at 22 ± 2°C with 50–60% humidity with free access to food and water before experiments. Animals were randomly assigned to either the control group or the AR group (n = 6 for each group). Adjuvant solutions were prepared by mixing ovalbumin (OVA, 10 μg/500 μl) and aluminum hydroxide ($Al(OH)_3$) (1 mg/500 μl). Mice in AR groups were then intraperitoneally injected with 200 μl adjuvant mixture on day 0, 7 and 14 (Yu et al. 2021). On day 21, OVA nasal drops (containing 500 μg OVA) were dropped into bilateral nasal cavities of mice for 7 days. Mice in control group received the same volume of saline. The number of sneezes and nasal rubbing episodes was recorded to evaluate whether AR was successfully induced. At the end of experiments, mice were anesthetized and eyeball blood was collected for separate serum. Then, the mice were sacrificed by cervical dislocation within 24 h after the last OVA exposure, and nasal mucosal tissues were collected and stored at −80°C.

Hematoxylin and eosin (H&E) staining

The nasal mucosal tissues of the mice were fixed with 4% paraformaldehyde (Solarbio, China) and embedded in paraffin. The paraffin-embedded tissues were cut into slides with 4-μm thickness, and then slides were dewaxed using xylene and rehydrated with descending concentration of ethanol. Following this, H&E staining was performed by using haematoxylin solution for 5 min and 0.5% eosin (Esebio Biotechnology Co., Ltd., Shanghai, China) for 1 min. Pathological changes were examined under a microscope (Nikon, Japan).

Enzyme-linked immunosorbent assay (ELISA)

Blood samples were centrifuged at 4000 rpm for 10 min at 4°C to separate serum samples. The levels of serum IgE, tumor necrosis factor-alpha (TNF-α), interleukin (IL-4), and interleukin (IL-5) were measured using ELISA kits as recommended by the instructions (Esebio Biotechnology Co., Ltd, China). The absorbance (OD value) was obtained at 450 nm using a microplate reader (Thermo Fisher Scientific, Pittsburgh, USA).

Cell culture and cell transfection

Primary mouse nasal mucosal epithelial cells (MIC-iCell-m024; cells free of mycoplasma infection) were purchased from icell Bioscience Inc. (Shanghai, China) and maintained in DMEM/F12 medium, supplemented with 10% fetal bovine serum (Gibco, USA), 1% streptomycin and 1% penicillin (Invitrogen, USA) at 37° with 5% CO_2. Lentiviral particles for transfection were obtained from Suzhou Jima Gene Co., Ltd (Suzhou, China). MIC-iCell-m024 cells were divided into 6 groups: (1) control group: cells were cultured under normal conditions without any additional treatment; (2) TNF-α-treated group (TNF-α group): AR model was induced by TNF-α as previously reported (Huang et al. 2021). When cells reached 70–80% confluence, TNF-α (10 ng/ml) was added into MIC-iCell-m024 cells for 24 h to induce AR; (3) GZMA silencing negative control group (TNF-α+si-NC group): TNF-α-treated MIC-iCell-m024 cells were transfected with a GZMA inhibitor negative control; (4) GZMA silencing group (TNF-α+si-GZMA): TNF-α-treated MIC-iCell-m024 cells were transfected with a GZMA inhibitor; (5) GZMA overexpression negative control group (TNF-α+oe-NC): TNF-α-treated MIC-iCell-m024 cells were transfected with a GZMA over-expression negative control vector; (6) GZMA overexpression group (TNF-α+oe-GZMA): TNF-α-treated MIC-iCell-m024 cells were transfected with

a GZMA overexpression vector. After transfection for 48 h, cells were collected for further analysis.

Cell viability

Cell Counting Kit-8 (CCK-8) assays were employed to evaluate cell viability. MIC-iCell-m024 cells (1×10^4 cells/well) were seeded in 96-well plates and incubated for 24 h, 48 h and 72 h at 37°C. Subsequently, 10 μl of CCK-8 solution (Beyotime, China) was added into each well, and cells were incubated at 37°C for 4 h. The absorbance was measured at 450 nm using a microplate reader (Thermo Fisher Scientific, USA).

5-ethynyl-2'-deoxyuridine (EdU) assay

The Edu assay can quantitatively measure the cell proliferation rates. In this study, cell proliferation after GZMA silencing was assessed using the EdU assay, based on Cell-Light EdU DNA Cell Proliferation Kit (RiboBio, China). MIC-iCell-m024 cells (1×10^4 cells/well) were seeded in 96-well plates and labeled with EdU (10 μmol/l) at 37°C for 2 h. Then, 4% paraformaldehyde (Solarbio, Beijing China) was used to fix cells, and 0.3% Triton X-10 was utilized to penetrate cells for 3 min, followed by nucleus staining with DAPI for 3 min. Positive staining cells were observed under an Olympus IX73 microscope (Olympus, Tokyo, Japan). Five groups of cells were randomly selected for counting, and the EDU-positive cell rate was calculated by ImageJ software.

Cell apoptosis

The effect of silencing GZMA on cell apoptosis was further assessed by Annexin V-FITC/propidium iodide (PI) Apoptosis Detection Kit (Vazyme, China). MIC-iCell-m024 cells (3×10^5 cells/well) were inoculated in 6-well plates and then stained with FITC-labeled Annexin V (5 μl) and PI (5 μl) for 15 min in the dark at room temperature. The apoptotic cells were detected by a cytometer (Beckman Coulter) and apoptosis rate was analyzed using Flowjo software (Tree Star, USA).

Quantitative reverse-transcription polymerase chain reaction (qRT-PCR)

Total RNA was extracted from nasal mucosal tissues and MIC-iCell-m024 cells by Trizol (Invitrogen, USA). The extracted RNAs were reverse transcribed into cDNA based on Hiscript II QRT Supermix for qPCR kits (Vazyme, China). The ChamQ Universal SYBR kit (Vazyme, China) was applied on ABI7500 system (Applied Biosystems) to conduct qRT-PCR program with the thermocycler conditions: an initial denaturation at 95°C for 10 min, followed by 36 cycles of denaturation at 95°C for 10 s and annealing at 60°C for 30 s. GAPDH served as an internal control, and we calculated the relative expression using $2^{-\Delta\Delta CT}$ method. The primers sequences for qRT-PCR are detailed in Supplementary material (Table S1).

Western blotting

RIPA buffer (Biosharp, China) was utilized to separate total proteins from nasal mucosal tissues and MIC-iCell-m024 cells. Pierce BCA kit was employed to determine the concentration of proteins. Next, proteins were separated by 10% sodium dodecyl-sulfate polyacrylamide gel electrophoresis (SDS-PAGE), and transferred onto polyvinylidene difluoride (PVDF) membranes for 1 h, and then blocked with 5% non-fat milk for 2 h at room temperature. After blocking, the membranes were incubated with primary antibodies against GZMA (1:200, sc-33692), p-JAK2 (1:1000, #3771, CST), JAK2 (1:100, sc-390539), p-STAT1 (1:200, sc-8394) and STAT1 (1:200, sc-464) overnight at 4°C. Following this, HRP-labeled secondary antibodies (1:2000, ab205718, Abcam) were incubated with membranes for 1 h at room temperature. GAPDH served as the internal control. Color was developed using enhanced chemiluminescence (ECL) luminescence reagent on Tanon 5200 system, and proteins were evaluated by ImageJ software.

Statistics

GraphPad Prism 7.0 (GraphPad Prism Software Inc., San Diego, California, USA) was employed to process experimental data. Results were expressed as means ± standard deviation (SD). Differences between two groups were compared using *t*-tests. One-way analysis of variance (ANOVA), followed by the Tukey's multiple comparisons test was utilized for comparisons among multiple groups. $p < 0.05$ was regarded as statistical meaningful.

Results

Identification of DEGs between AR and non-allergic controls

Before analysis, data was normalized and the distribution of samples in GSE18574 and GSE43523 datasets was displayed using boxplots. The results indicated that the normalized data was well-aligned (Fig. 1A,B). Subsequently, differential expression analysis was performed to screen for DEGs in the two datasets. Under the threshold of $p < 0.05$ and $|\log2FoldChange| \geq 0.5$, a total of 2607 DEGs were identified in GSE18574 dataset, comprising 1059 upregulated genes and 1548 downregulated genes (Fig. 1C). In GSE43523 dataset, we identified 431 DEGs, including 219 upregulated genes and 212 downregulated genes (Fig. 1D). According to the threshold, we displayed the top 15 upregulated and down-

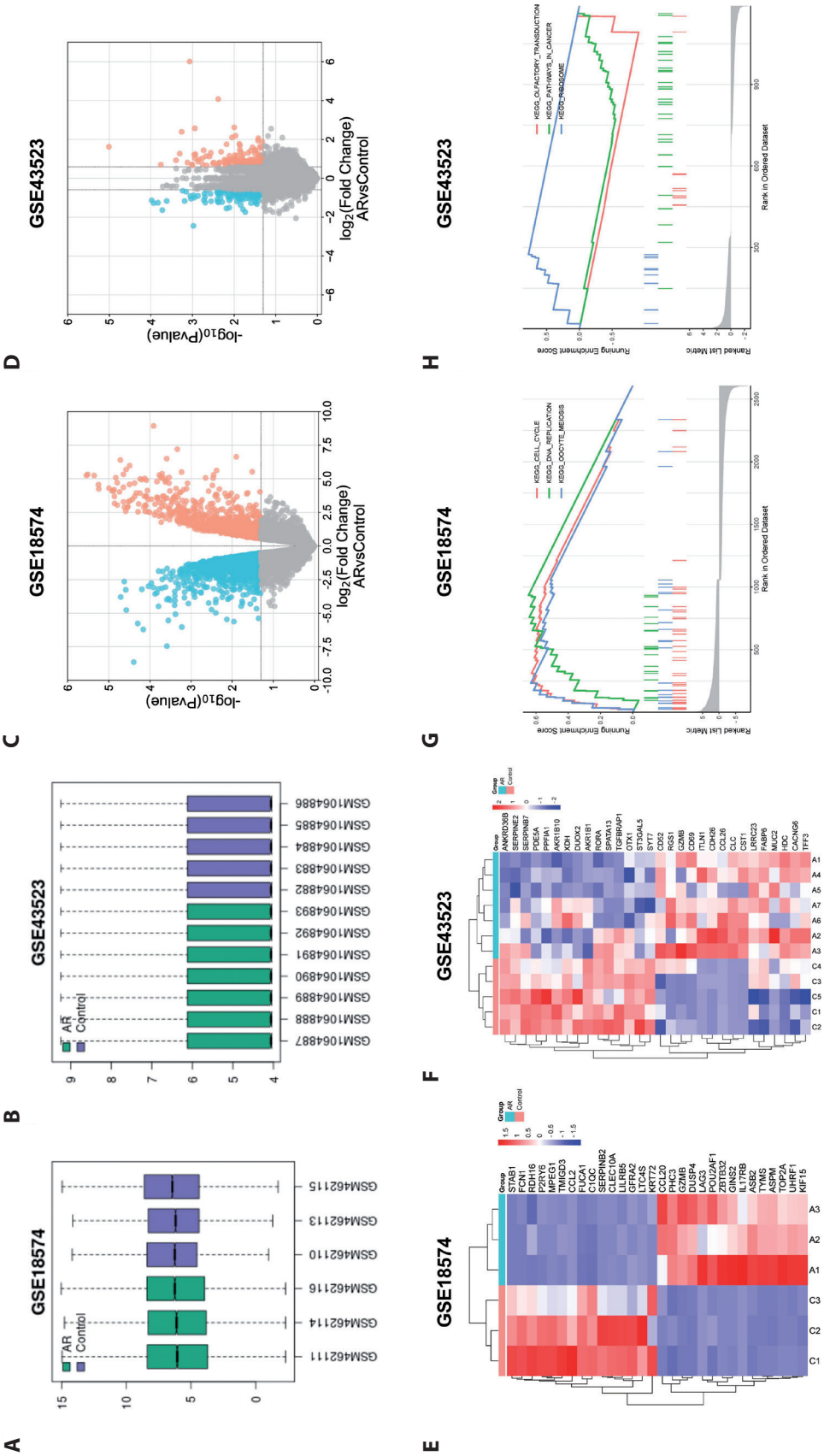

Figure 1. Screening DEGs between AR and non-allergic controls. **A,B.** Box plots for data distribution in GSE18574 and GSE43523 datasets. **C,D.** Volcano plots show DEGs in GSE18574 and GSE43523 datasets. Blue plots represent downregulated genes and orange ones represent upregulated genes. **E,F.** Expression patterns for top 15 upregulated and downregulated genes in GSE18574 and GSE43523 datasets. **G,H.** GSEA reveals the significantly enriched biological pathways for DEGs in GSE18574 and GSE43523 datasets. AR, allergic rhinitis; DEGs, differentially expressed genes; GSEA, gene set enrichment analysis.

regulated genes in both GSE18574 and GSE43523 datasets in Table S2 and S3. Figure 1E and F showed the expression patterns for the top 15 DEGs. To interpret DEGs in the two datasets, GSEA was employed to determine significantly biological pathways for DEGs. DEGs in GSE18574 dataset were mainly enriched in cell cycle, DNA replication and oocyte meiosis (Fig. 1G); DEGs in GSE43523 dataset were abundant in olfactory transduction, pathways in cancer and ribosome pathways (Fig. 1H).

Co-DEGs and functional enrichment analyses

We drew a Venn diagram to obtain the co-DEGs between GSE18574 and GSE43523 datasets, discovering 68 co-DEGs at their intersection (Fig. S1 in Supplementary material). Next, these 68 co-DEGs were subjected to GO and KEGG enrichment analyses. The top 10 GO terms were shown in Figure 2A–C. In MF category, co-DEGs were mainly enriched in steroid binding, sterol binding, proteasome binding, protein disulfide isomerase activity, intramolecular oxidoreductase activity, transposing S-S bonds, steroid hormone receptor activity, and sterol transporter activity. In BP category, co-DEGs were abundant in protein acylation, regulation of chromatin organization, cellular response to sterol, protein acetylation, cytolysis, protein autophosphorylation, histone H3-K9 methylation, and regulation of I-kappaB kinase/NF-kappaB signaling. In MF category, peptidase complex, immunological synapse, proteasome complex, endopeptidase complex, and ATPase complex were the significant GO terms. Additionally, co-DEGs were significantly involved in nucleotide excision repair, adrenergic signaling in cardiomyocytes, MAPK signaling pathway, and inflammatory bowel disease (Fig. 2D).

Determination and analysis of hub genes

In order to understand the interactions among gene-coded proteins involved in AR, we constructed a PPI network (Fig. 3A) and determined top 5 genes (HIST1H2BD, RPS28, HIST1H1C, MAF and GZMA) as hub genes according to the degree of each protein node (Fig. 3B). Furthermore, box plots were drawn to show changes of hub gene expression within GSE43523 dataset. As shown in Figure 4A, HIST1H2BD (p = 6.2e−5), RPS28 (p = 0.06), HIST1H1C (p = 0.02) and GZMA (p = 0.03) were upregulated in AR, while MAF (p = 0.04) was downregulated in AR. Ridgeline plots were also drawn in order to examine the distribution of hub genes in samples. Ridgeline plots displayed that the expression distribution

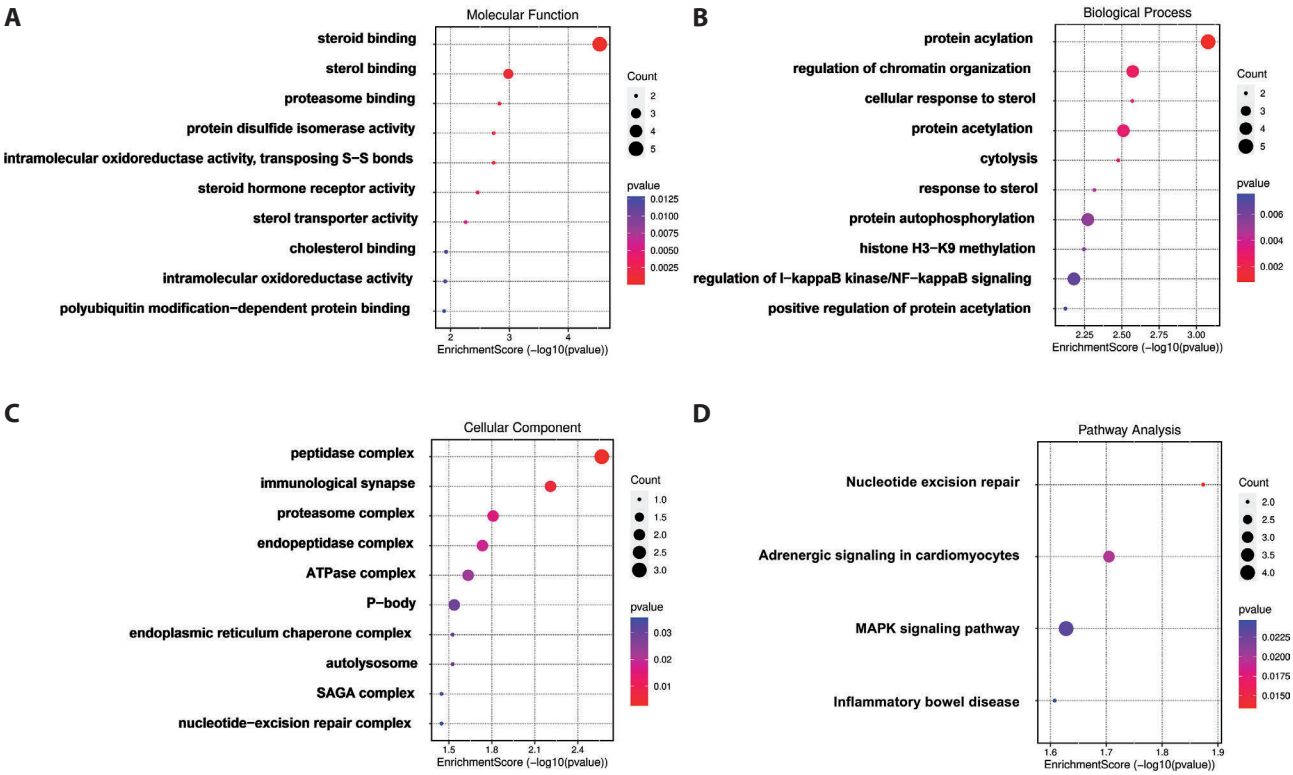

Figure 2. Functional enrichment analysis for co-DEGs. Bubble diagrams for the top 10 GO terms in BP (**A**), CC (**B**), and MF (**C**) categories. **D.** Bubble diagrams for KEGG enrichment analysis. co-DEGs, common differentially expressed genes; BP, biological process; CC, cellular component; MF, molecular function; KEGG, Kyoto Encyclopedia of Genes and Genomes.

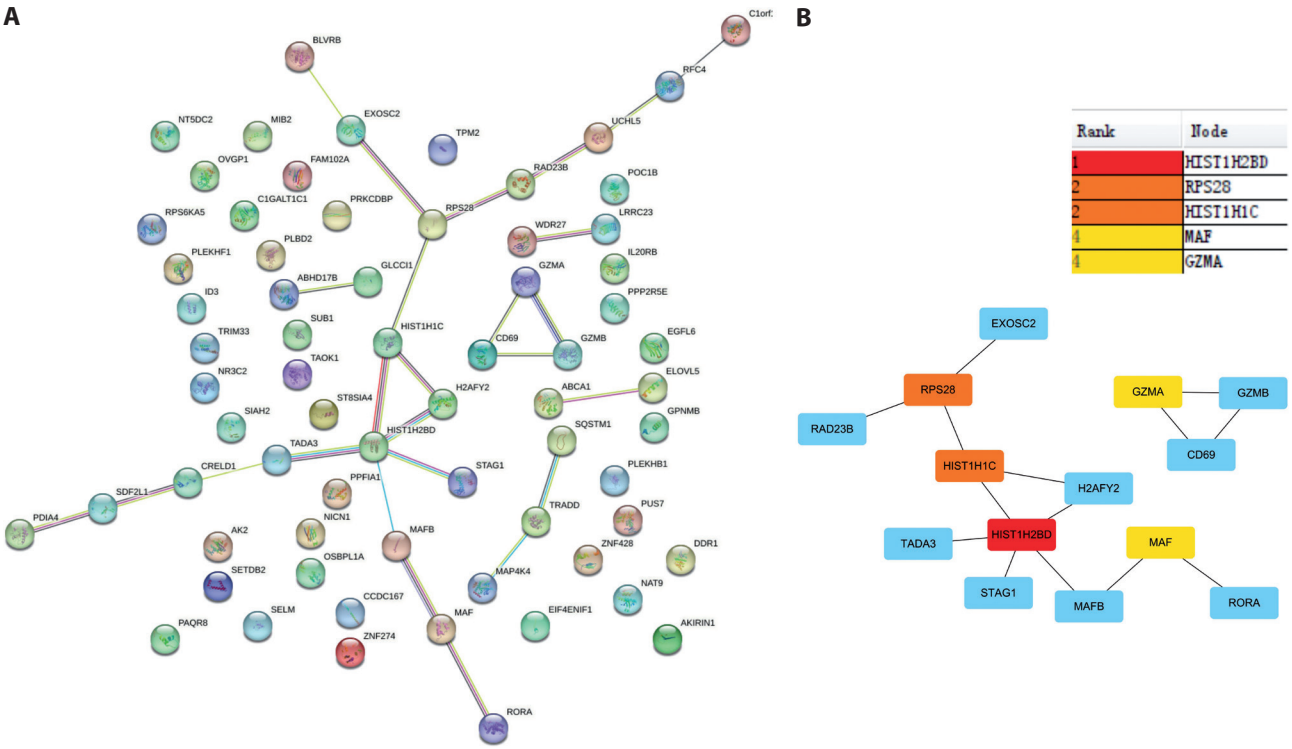

Figure 3. Construction of a PPI network and identification of hub genes. **A.** The PPI network. **B.** The top 5 genes (HIST1H2BD, RPS28, HIST1H1C, MAF and GZMA) as hub genes. PPI, protein-protein interaction network.

was relatively concentrated for each hub gene (Fig. 4B). Then, a correlation heatmap was generated to demonstrate the correlation of hub genes (Fig. 4C). HIST1H2BD was positively correlated with RPS28, HIST1H1C and GZMA, whereas MAF was negatively correlated with RPS28. Besides, PCA showed that the application of hub genes might distinguish control and AS (Fig. 4D). To verify the classification efficiency of hub genes in differentiating AR patients from healthy controls, ROC curves were further generated using in GSE43523 dataset. Figure 5 displayed that the 5 hub genes exhibited good performance in distinguishing AR and control, with AUC great than 0.800.

GZMA is highly expressed in OVA-induced AR mice

GZMA was selected for further experimental studies. We constructed an AR mouse model induced by OVA, and measured the frequency of nasal sneezing and nasal rubbing. As displayed in Figure 6A, OVA-induced AR mice exhibited increased frequencies of sneezing and nasal rubbing than that of control mice ($p < 0.01$). Furthermore, H&E staining revealed that the nasal mucosa was intact and devoid of inflammation in the control group. In contrast, AR mice exhibited obvious tissue edema, disrupted and dislodged cilia, and dilation of small blood vessels, with an increased number of cupped cells carrying secretory bodies, and inflammatory cell infiltration (Fig. 6B). Meanwhile, the levels of serum IgE, TNF-α, IL-4 and IL-5 were detected by ELISA (Fig. 6C,D). The levels of IgE, TNF-α, IL-4 and IL-5 were remarkably elevated in AR mice compared to control mice ($p < 0.01$). These results implied that OVA-induced AR had been successfully established. To quantify the expression of GZMA, qRT-PCR and Western blot analysis were employed in OVA-induced AR mice. The mRNA expression of GZMA was significantly upregulated in AR mice compared with control mice ($p < 0.01$) (Fig. 6E). The similar results were also observed in Western blot analysis (Fig. 6F).

GZMA influences inflammation, cell viability, proliferation, and apoptosis in TNF-α-induced MIC-iCell-m024 cells

In MIC-iCell-m024 cells, TNF-α (10 ng/ml) was applied to induce AR, and the level of GZMA was apparently increased after TNF-α exposure compared to the control group ($p < 0.01$), whereas silencing GZMA significantly decreased its expression compared to the TNF-α+si-NC group ($p < 0.01$) (Fig. 7A). Since si-GZMA-1 demonstrated a more stable knockdown efficiency, it was chosen for subsequent experiments. Additionally, GZMA was highly expressed in MIC-iCell-m024 cells after overexpression of GZMA (Fig. 7B). Figure 7C revealed that TNF-α expo-

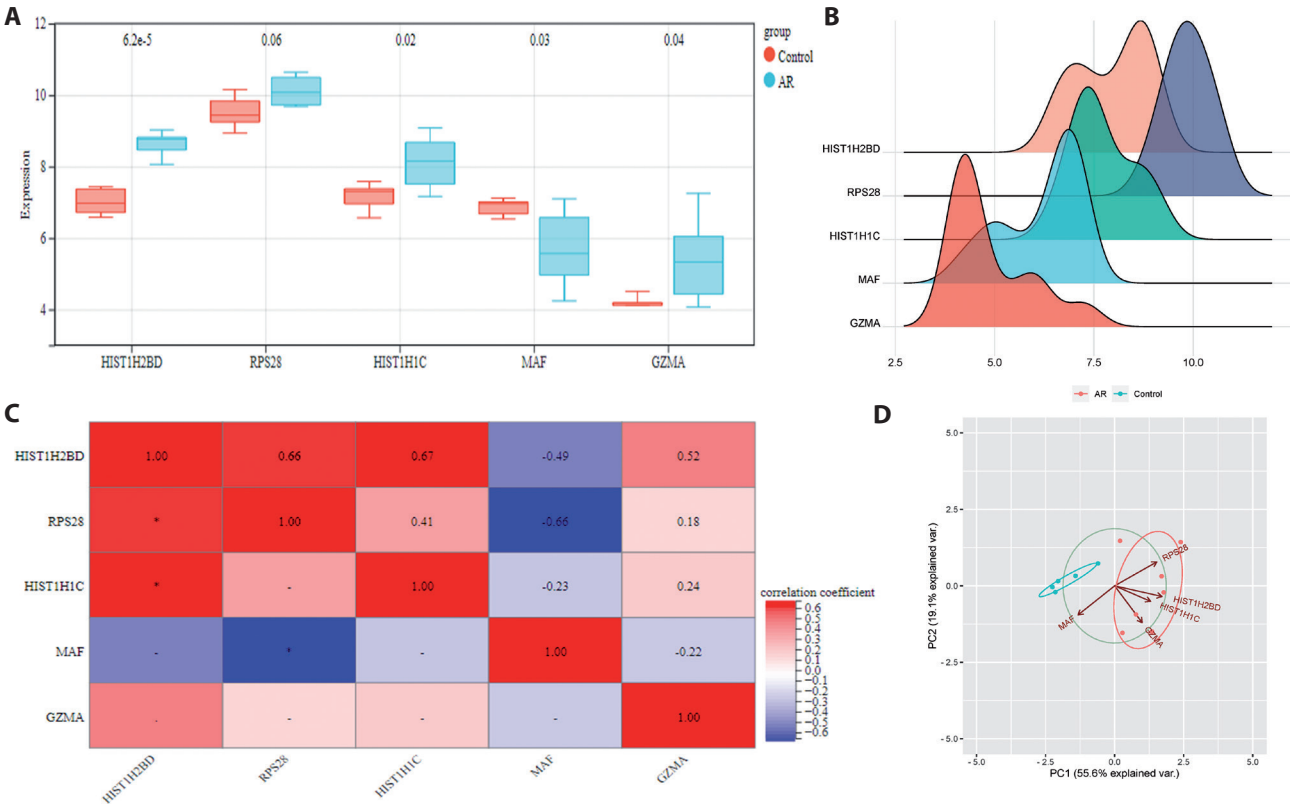

Figure 4. Analysis of hub genes. **A.** Box plots show hub gene expression in GSE43523 dataset. **B.** Ridgeline plots examine the distribution of hub genes. **C.** Visualization of the association matrices for hub genes. **D.** PCA shows the separation of AR and controls by application of hub genes in GSE43523 dataset. PCA, principal components analysis; AR, allergic rhinitis.

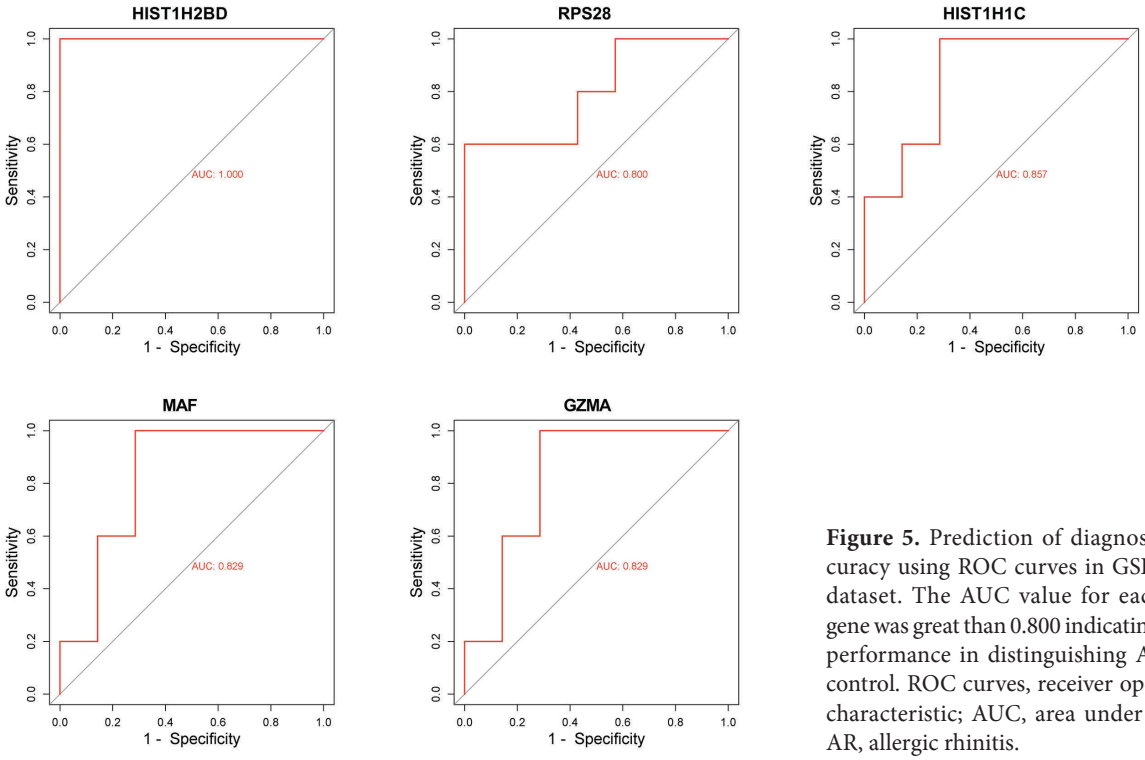

Figure 5. Prediction of diagnostic accuracy using ROC curves in GSE43523 dataset. The AUC value for each hub gene was great than 0.800 indicating good performance in distinguishing AR and control. ROC curves, receiver operating characteristic; AUC, area under curve; AR, allergic rhinitis.

sure promoted the production of IL-6, IL-4 and IL-5 compared to the control group ($p < 0.01$). However, silencing GZMA decreased TNF-α-induced production of IL-6, IL-4 and IL-5 ($p < 0.01$). In contrast, overexpression of GZMA promoted IL-6, IL-4, and IL-5 levels in TNF-α-treated MIC-iCell-m024 cells ($p < 0.01$). Compared to the control group, TNF-α application also reduced cell viability ($p < 0.01$), whereas silencing GZMA significantly increased cell viability ($p < 0.01$) (Fig. 7D). Besides, an Edu assay was used to assess the effect of silencing and overexpression of GZMA on MIC-iCell-m024 cells. A decreased cell proliferation rate was found in TNF-α group compared to the control group ($p < 0.01$); whereas, silencing GZMA enhanced cell proliferation rate compared to the TNF-α+si-NC group ($p < 0.01$) (Fig. 7E). Moreover, GZMA overexpression further augmented the reduction in cell viability and proliferation induced by TNF-α treatment ($p < 0.01$) (Fig. 7D,E). Additionally, we measured the apoptotic cells caused by silencing and overexpression of GZMA using flow cytometry. Silencing GZMA significantly repressed TNF-α-induced cell apoptosis in MIC-iCell-m024 cells ($p < 0.01$). Contrarily, overexpression of GZMA further facilitated apoptosis in TNF-α-treated MIC-iCell-m024 cells ($p < 0.01$) (Fig. 7F). Collectively, these findings suggest that silencing GZMA could promote cell viability and proliferation but inhibiting cell apoptosis in TNF-α-induced MIC-iCell-m024 cells, while GZMA overexpression played the opposite roles, which suggested that silencing GZMA was protective for TNF-α-induced AR by enhancing survival of MIC-iCell-m024 cells.

Silencing GZMA represses the JAK2/STAT1 pathway

The JAK/STAT is an important signaling pathway regulated by cytokines and plays an important role in inflammation and autoimmune diseases (Xue et al. 2023). Therefore, we investigated the effects of GZMA silencing on JAK2/STAT1 pathway in MIC-iCell-m024 cells. The results from Western blot analysis demonstrated that TNF-α exposure triggered the expression of p-JAK2 and p-STAT1 compared to the control group ($p < 0.01$), while silencing GZMA reversed the effect of TNF-α on JAK2/STAT1, which was evidenced by downregulated p-JAK2/

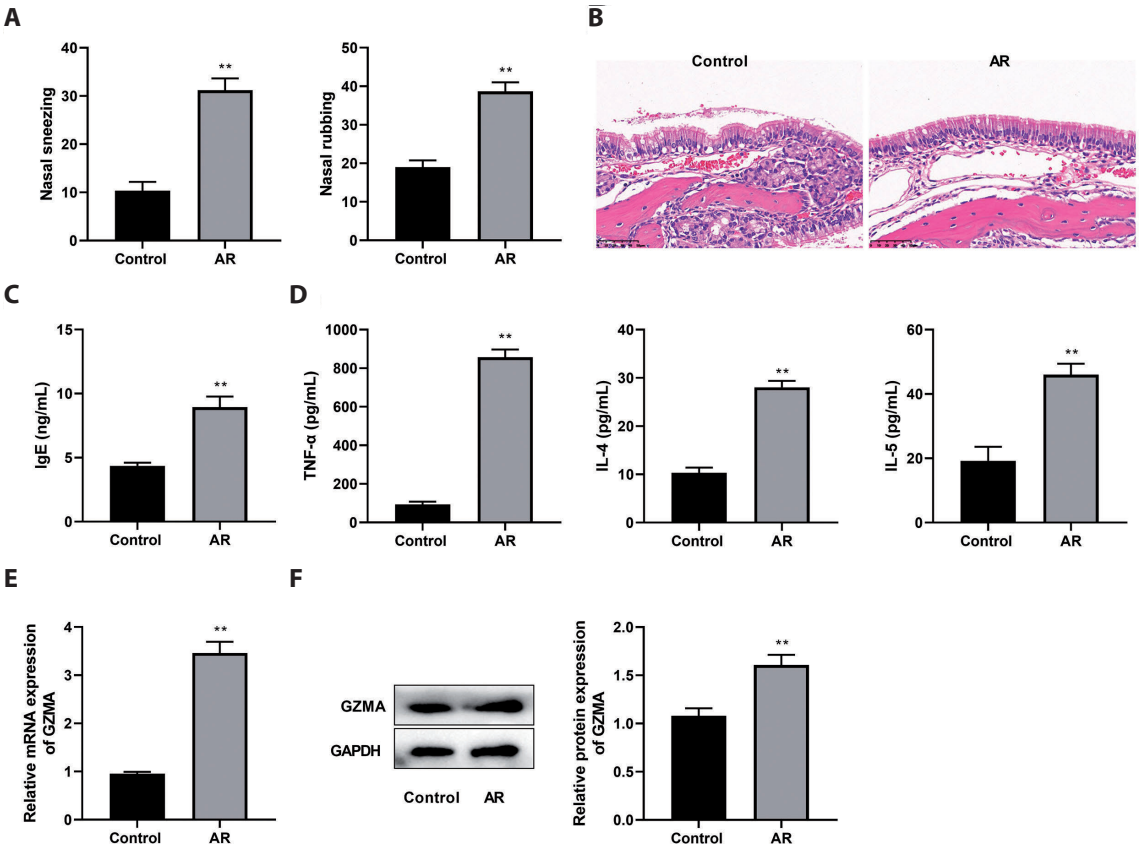

Figure 6. GZMA is highly expressed in OVA-induced AR mice. **A.** The rate of nasal sneezing and nasal rubbing is increased in OVA-induced AR mice. **B.** Pathological examination using H&E staining for nasal mucosal tissues of mice. **C, D.** ELISA for detection of serum levels of IgE, TNF-α, IL-4 and IL-5 in OVA-induced AR mice. qRT-PCR (**E**) and Western blot (**F**) analysis are employed to quantify the expression of GZMA in OVA-induced AR mice. ** $p < 0.01$, *vs.* control group. OVA, ovalbumin; AR, allergic rhinitis; H&E staining, hematoxylin and eosin staining; ELISA, enzyme-linked immunosorbent assay; qRT-PCR, quantitative reverse-transcription polymerase chain reaction.

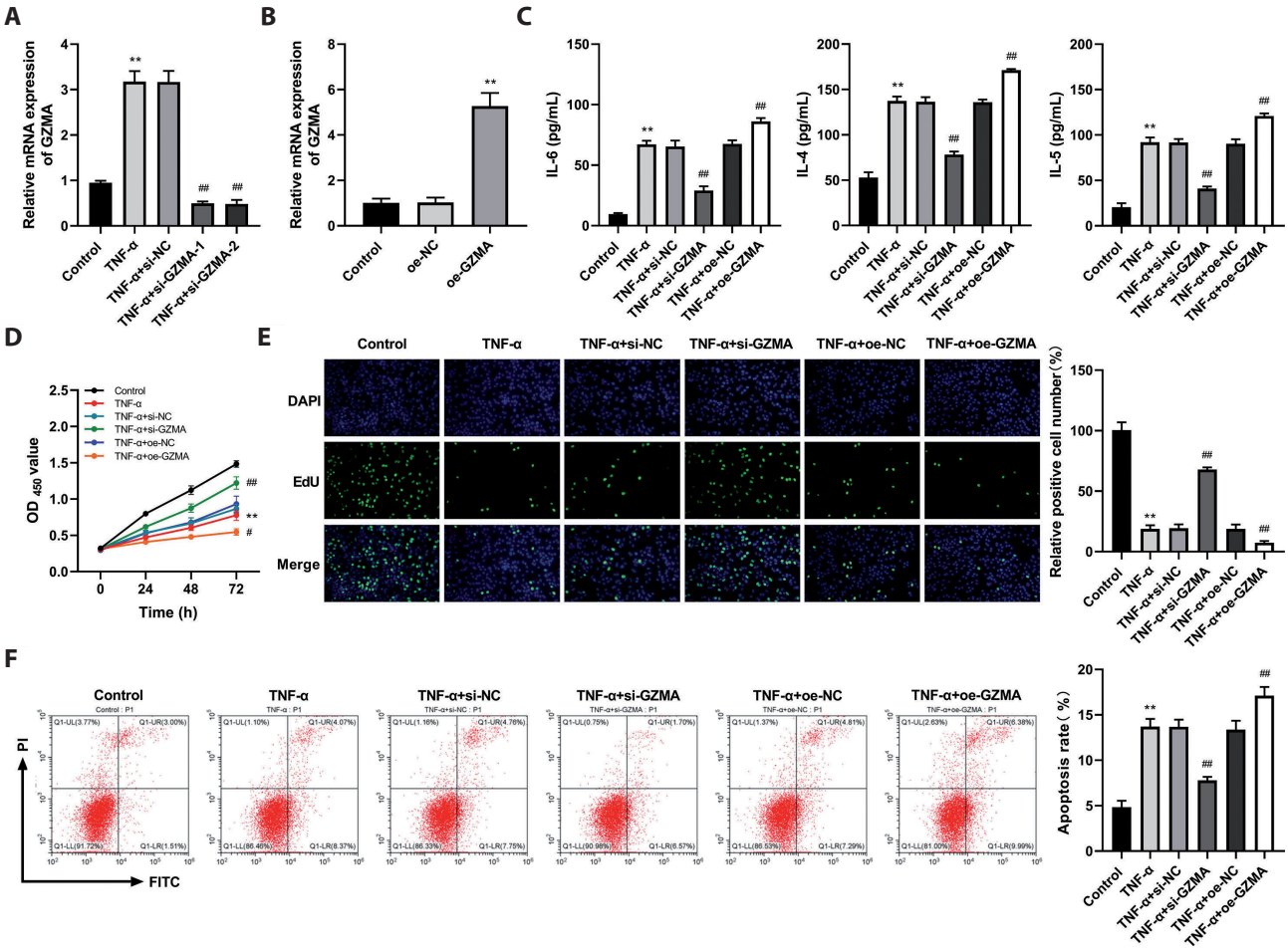

Figure 7. GZMA affects inflammation response, cell viability, proliferation, and cell apoptosis in TNF-α-induced MIC-iCell-m024 cells. **A,B.** qRT-PCR quantifies the expression level of GZMA after transfection with si-GZMA-1, si-GZMA-2, and oe-GZMA in TNF-α-induced MIC-iCell-m024 cells. **C.** ELISA for detection of serum levels of IL-6, IL-4 and IL-5 in TNF-α-induced MIC-iCell-m024 cells. **D.** CCK-8 assay measures cell viability after silencing or overexpressing GZMA in TNF-α-induced MIC-iCell-m024 cells. **E.** EdU assay evaluates cell proliferation after silencing or overexpressing GZMA in TNF-α-induced MIC-iCell-m024 cells. **F.** Apoptosis is determined by flow cytometry after silencing or overexpressing GZMA in TNF-α-induced MIC-iCell-m024 cells. ** $p < 0.01$, *vs.* control group. ## $p < 0.01$, *vs.* TNF-α+si-NC group. qRT-PCR, quantitative reverse-transcription polymerase chain reaction; ELISA, enzyme-linked immunosorbent assay; CCK-8, cell counting kit-8 assay; EdU, 5-ethynyl-2'-deoxyuridine.

JAK2 and p-STAT1/STAT1 (Fig. 8). The results suggested that silencing GZMA repressed JAK2/STAT1 pathway.

Discussion

Allergic rhinitis (AR) is prevalent worldwide due to unhealthy lifestyle and environmental pollution. Novel specific and sensitive biomarkers as well as potential mechanisms are urgent to be identified for the pathogenesis, diagnosis and treatment of AR. Hence, we determined 5 hub genes HIST1H2BD, RPS28, HIST1H1C, MAF and GZMA associated with AR, and we found their significant diagnostic value in differentiating AR from control samples. Furthermore, we observed that GZMA was highly expressed in OVA-induced AR mice. Silencing GZMA promoted cell viability and proliferation but inhibited cell apoptosis and inflammatory responses in TNF-α-induced MIC-iCell-m024 cells. On the contrary, the overexpression of GZMA elicited the opposite effects. Additionally, silencing GZMA inhibited the JAK2/STAT1 signaling pathway.

Previous studies have unveiled that histone family H2B genes are differentially expressed across various cell lines, hinting at the influence of specific cellular circumstances on the polyadenylation of replication-dependent histone (pARDH) (Kari et al. 2013). Guo has found that HIST1H2BD (Histone H2B type 1-D) and HIST1H1C (Histone H1.2) as

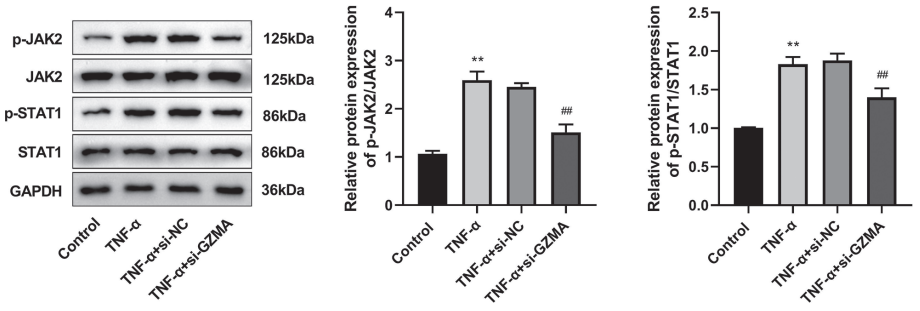

Figure 8. Silencing GZMA represses JAK2/STAT1 pathway. Western blot analysis quantifies the protein levels of p-JAK2/JAK2 and p-STAT1/STAT1 in TNF-α-induced MIC-iCell-m024 cells. ** $p < 0.01$, *vs.* control group. ## $p < 0.01$, *vs.* TNF-α+si-NC group.

pRDH, and RNA virus infection causes abnormal pRDH levels leading to inflammatory response or cellular senescence (Guo et al. 2023). Excessive level of HIST1H1C promotes autophagy, inflammation and cell toxicity during diabetic retinopathy development (Wang et al. 2017). Meanwhile, RPS28 (40S ribosomal protein S28) encodes a ribosomal protein serving as a component of 40S subunit, and has been identified as a DEG associated with oxidative phosphorylation and the ribosome pathway, contributing to inflammation progression (Li et al. 2022). Sun has demonstrated that MAF (MAF BZIP Transcription Factor) reduces inflammation by improving the balance of Th1/Th2/Th17 and epithelial barrier function, thereby ameliorating OVA-induced AR (Sun et al. 2022). This study first identified GZMA, HIST1H2BD, RPS28, HIST1H1C and MAF as hub genes that were associated with the pathogenesis of AR. Furthermore, we found these hub genes exhibited excellent performance in distinguishing between AR and control, with an AUC greater than 0.800. Therefore, this study might provide potential biomarkers for pathogenesis, diagnosis and therapeutics of AR. Subsequently, we chose GZMA, which had a stronger correlation with immune and inflammatory responses (Moreno-Martinez et al. 2022), for further exploration.

By interacting with perforin, GZMA exhibits cytotoxic properties to eliminate tumor or virus-infected cells. However, when GZMA is present without perforin, it promotes inflammation and triggers various immune cells (Shimizu et al. 2019). Hewagama has found GZMA as one of the inflammatory/cytotoxic genes in re-stimulated T cells, contributing to female autoimmune diseases, which may explain the gender disparity observed in autoimmune diseases (Hewagama et al. 2009). Meanwhile, Th cells that product GZMA differentiation in the presence of IL-4, IL-6, and IL-21; STAT3 and STAT6 are crucial for the differentiation of Th cells producing GZMA. Notably, Th cells producing GZMA are implicated in the incidence and poor outcome of acute graft-*versus*-host disease (Park et al. 2020). In the present study, we first demonstrated that silencing GZMA could promote cell viability and proliferation but inhibited cell apoptosis in TNF-α-induced MIC-iCell-m024 cells. Contrarily, overexpression of GZMA brought about opposite effects.

The study has indicated that JAK-STAT pathway contributes to chronic inflammation and pruritus in atopic dermatitis by regulating Th2 cytokines, including IL-4, IL-5, IL-13, IL-31, and thymic stromal lymphopoietin (Huang et al. 2022). Elevated levels of Th2-originated cytokines, such as IL-4 and IL-5, are critical in the immune response of the nasal mucosa among AR patients. Recently, Nur Husna and colleagues have revealed that elevated serum IL-4/IL-13 may involve in decreased tight junction molecules expression through IL-4Rα/IL-13Rα1 heterodimeric receptor, providing novel insights into the pathogenesis of AR (Nur Husna et al. 2022a). Meanwhile, compelling evidence has suggested that normal bone marrow eosinophilia requires IL-5 to respond to specific sensitization in the process of AR; whereas, inhibition of IL-5-mediated eosinophil pathway cannot absolutely alleviate AR symptoms or nasal histamine hyperresponsiveness, indicating that there are other cytokine-progenitor pathways participating in various inflammatory responses (Saito et al. 2002). Furthermore, IL-6 promotes the differentiation of activated B cells into Ig-producing cells and regulates the direction of specific differentiation of initial CD4+ T cells in the acquired immune response (Kimura et al. 2010). Certain biological agents, such as dupilumab targeting IL-4 receptor, omalizumab targeting IgE, as well as mepolizumab, reslizumab and benralizumab targeting IL-5, have been reported to improve chronic rhinosinusitis with nasal polyposis (Geng et al. 2021). The USP7-STAT3-granzyme-Par-1 axis is crucial in regulating allergic inflammation through enhancing the differentiation of IL-5-producing Th2 cells, and targeting this pathway may represent a viable approach to ameliorate intractable allergic inflammation (Kumagai et al. 2023). IL-9 signaling represses the increase in intestinal GZMA in CD4+ T cells, indicating a regulatory role for IL-9 in controlling GZMA levels during allergic reactions (Hayes et al. 2020). Previous investigations have found that GZMA promotes the levels of IL-6, IL-4 and IL-5 in AR, all of which activate the JAK/STAT signaling pathway (Gandhi et al. 2016; Aliyu et al. 2022; Shankar et al. 2022). In this study, we evaluated the effect of silencing GZMA on the production of IL-4, IL-5, and IL-6 in TNF-α-induced AR, and we found that silencing GZMA significantly decreased the levels of IL-4, IL-5, and IL-6. Furthermore, we observed

that GZMA silencing decreased the ratio of p-JAK2/JAK2 and p-STAT1/STAT1, indicating the inhibition of JAK2/STAT1 pathway. These results implied the important role of GZMA in the regulation of allergic inflammation.

The dysregulation of JAK-STAT induces autoimmune diseases, including rheumatoid arthritis, ulcerative colitis, and Crohn disease. Additionally, aberrant JAK-STAT signaling contributes to the pathogenesis of myelofibrosis, polycythemia vera, and myeloproliferative illnesses (Roskoski Jr. 2016). It has been noticed that JAK2 variant signaling is associated with genetic, hematological and immunological implication in chronic myeloproliferative neoplasms (Torres et al. 2022). Clinically, some inhibitors of the JAK/STAT signaling pathway have been used to treat allergic disorders. For example, tofacitinib, a non-selective JAK inhibitor, is used in rheumatoid arthritis, psoriatic arthritis, polyarticular juvenile idiopathic arthritis, and ulcerative colitis. Abrocitinib and ruxolitinib have been approved for the atopic dermatitis treatment (Eisenman et al. 2022). A Pooled safety analysis has revealed that adult atopic dermatitis patients who received baricitinib treatment have a low incidence of serious infections, opportunistic infections and conjunctival disorders, without malignant tumors, gastrointestinal perforations, positively cardiovascular events or tuberculosis (Bieber et al. 2021). Moreover, Zak has found that JAK1 may be the most crucial isoform for IL-13 signaling, and JAK inhibition may provide an alternative small molecule approach to blocking IL-13 signaling, which could help develop topical drugs for treating IL-13 mediated allergic disorders (Zak et al. 2019). Besides, other small molecule cytokine antagonists, such as inhibitors targeting phosphodiesterase 4 and T-helper 2 cells (CRTH2), show potential in the treatment of allergic diseases (Howell et al. 2018). This novel therapy may provide benefits to patients with allergic diseases by targeting specific inflammatory pathways in the pathogenesis of these diseases. In this study, we found that inhibition of the JAK2/STAT1 signaling pathway by silencing GZMA might be beneficial for AR, offering novel insights into the amelioration of AR.

Nevertheless, limitations should be addressed in the present study. We downloaded expression profiling data of seasonal AR patients from the GEO database and identified DEGs by bioinformatics analysis. Yet, the limited sample size might have induced inaccuracies in our results. Thus, RNA-sequencing analysis with a larger sample size is essential to validate the findings. Besides, we only selected GZMA for experimental studies to evaluate its role in AR and JAK2/STAT1 pathway, while the effects of other hub genes on AR remain unexplored. Further experimental studies should be carried out to investigate the functions in AR. Moreover, while the diagnostic value of hub genes in distinguishing AR from control has been assessed using ROC curves in this study, its reliability should be further validated by constructing prognostic models in an external validation cohort. Additionally, we selected male BALB/c mice for this study, and therefore it may introduce potential bias when considering their applicability to female AR patients. Then, the investigation of JAK-STAT signaling pathway involved the detection of changes in the expression of JAK-STAT-related proteins following the knockdown of GZMA. Future research will encompass in-depth in vitro and *in vivo* functional experiments to provide a comprehensive understanding.

Conclusion

To sum up, we determined 5 hub genes (HIST1H2BD, RPS28, HIST1H1C, MAF and GZMA) associated with AR within a PPI network. Furthermore, we successfully constructed an AR model by OA in mice and found that GZMA was highly expressed in OVA-induced AR mice. Silencing GZMA promoted cell viability and proliferation but inhibited cell apoptosis in TNF-α-induced MIC-iCell-m024 cells, whereas overexpression of GZMA exerted the opposite effects. Additionally, silencing GZMA repressed the JAK2/STAT1 pathway, which might provide theoretical supports for the management of AR.

Ethical approval. All methods are reported in accordance with ARRIVE guidelines for the reporting of animal experiments. The animal experiments conformed to the Guide for the Care and Use of Laboratory Animals. Animal study has been approved by the Animal Ethics Committee of Shanxi Bethune Hospital, Shanxi Academy of Medical Sciences, Third Hospital of Shanxi Medical University, Tongji Shanxi Hospital.

Conflict of interest. The authors declare that they have no conflicts of interest to disclose.

Authors' contributions. Conceptualization: LL and YZ; formal analysis: LL, YZ, JW, LZ, YG and FZ; investigation: LL and XJ; methodology: LL, XJ and TW; writing original draft: YZ, JW, LZ, YG, XJ, TW and FZ; writing review and editing: LL. Approval of final manuscript: all authors.

Funding. This work was supported by the Free Exploration youth scientific research Project of Shanxi Basic Research Program (No: 202203021212107).

Availability of data and materials. All data in the manuscript is available through the responsible corresponding author.

References

Aliyu M, Zohora FT, Anka AU, Ali K, Maleknia S, Saffarioun M, Azizi G (2022): Interleukin-6 cytokine: An overview of the immune regulation, immune dysregulation, and therapeutic approach. Int. Immunopharmacol. **111,** 109130 https://doi.org/10.1016/j.intimp.2022.109130

Bieber T, Thyssen JP, Reich K, Simpson EL, Katoh N, Torrelo A, De Bruin-Weller M, Thaci D, Bissonnette R, Gooderham M, et al. (2021): Pooled safety analysis of baricitinib in adult patients with atopic dermatitis from 8 randomized clinical trials. J. Eur. Acad. Dermatol. Venereol. **35,** 476-485 https://doi.org/10.1111/jdv.16948

Dong F, Tan J, Zheng YJM (2020): Chlorogenic acid alleviates allergic inflammatory responses through regulating Th1/Th2 balance in ovalbumin-induced allergic rhinitis mice. Med. Sci. Monit. **26,** e923358 https://doi.org/10.12659/MSM.923358

Eisenman D, Swindle S (2022): Food and drug administration guidance on design of clinical trials for gene therapy products with potential for genome integration or genome editing and associated long-term follow-up of research subjects. Appl. Biosaf. **27,** 201-209 https://doi.org/10.1089/apb.2022.0022

Franceschini A, Szklarczyk D, Frankild S, Kuhn M, Simonovic M, Roth A, Lin J, Minguez P, Bork P, Von Mering C (2012): STRING v9. 1: protein-protein interaction networks, with increased coverage and integration. Nucleic Acids Res. **41,** D808-D815 https://doi.org/10.1093/nar/gks1094

Gandhi NA, Bennett BL, Graham NM, Pirozzi G, Stahl N, Yancopoulos GD (2016): Targeting key proximal drivers of type 2 inflammation in disease. Nat. Rev. Drug Discov. **15,** 35-50 https://doi.org/10.1038/nrd4624

Geng B, Dilley M, Anterasian C (2021): Biologic therapies for allergic rhinitis and nasal polyposis. Curr. Allergy Asthma Reports **21,** 36 https://doi.org/10.1007/s11882-021-01013-y

Gotthardt D, Trifinopoulos J, Sexl V, Putz EM (2019): JAK/STAT cytokine signaling at the crossroad of NK cell development and maturation. Front. Immunol. **10,** 2590 https://doi.org/10.3389/fimmu.2019.02590

Grzegorczyk J, Kowalski ML, Pilat A, Iwaszkiewicz J (2002): Increased apoptosis of peripheral blood mononuclear cells in patients with perennial allergic asthma/rhinitis: relation to serum markers of apoptosis. Mediators Inflamm. **11,** 225-233 https://doi.org/10.1080/09629350290000087

Guo M, Zhu J, Hu Z, Wang Q, Songyang Z, Xiong Y (2023): Histone mRNA polyadenylation-mediated inflammation underlies various virus infections and cancers. J. Med. Virol. **95,** e28826 https://doi.org/10.1002/jmv.28826

Hattori H, Rosas LE, Okano M, Durbin JE, Nishizaki K, Satoskar AR (2007): STAT1 is involved in the pathogenesis of murine allergic rhinitis. Am. J. Rhinol. **21,** 241-247 https://doi.org/10.2500/ajr.2007.21.2970

Hayes TA, Ulrich BJ, Fu Y, Pajulas A, Kaplan MH (2020): IL-9 represses intestinal granzyme A positive CD4 T cells in mice with allergic airway inflammation. J. Immunol. **204,** 221.3 https://doi.org/10.4049/jimmunol.204.Supp.221.3

Hewagama A, Patel D, Yarlagadda S, Strickland FM, Richardson BC (2009): Stronger inflammatory/cytotoxic T-cell response in women identified by microarray analysis. Genes Immun. **10,** 509-516 https://doi.org/10.1038/gene.2009.12

Howell MD, Fitzsimons C, Smith PA (2018): JAK/STAT inhibitors and other small molecule cytokine antagonists for the treatment of allergic disease. Ann. Allergy Asthma. Immunol. **120,** 367-375 https://doi.org/10.1016/j.anai.2018.02.012

Hu X, Li J, Fu M, Zhao X, Wang W (2021): The JAK/STAT signaling pathway: from bench to clinic. Signal. Transduct. Target Ther. **6,** 402 https://doi.org/10.1038/s41392-021-00791-1

Huang H, Ren Y, Liang H, Liu X, Nan J, Zhao H, Liu X (2021): Mechanism of TCONS_00147848 regulating apoptosis of nasal mucosa cells and alleviating allergic rhinitis through FOSL2-mediated JAK/STAT3 signaling pathway. Sci. Rep. **11,** 15991 https://doi.org/10.1038/s41598-021-94215-3

Huang IH, Chung WH, Wu PC, Chen CB (2022): JAK-STAT signaling pathway in the pathogenesis of atopic dermatitis: An updated review. Front. Immunol. **13,** 1068260 https://doi.org/10.3389/fimmu.2022.1068260

Kari V, Karpiuk O, Tieg B, Kriegs M, Dikomey E, Krebber H, Begus-Nahrmann Y, Johnsen SA (2013): A subset of histone H2B genes produces polyadenylated mRNAs under a variety of cellular conditions. PloS One **8,** e63745 https://doi.org/10.1371/journal.pone.0063745

Kimura A, Kishimoto T (2010): IL-6: regulator of Treg/Th17 balance. Eur. J. Immunol. **40,** 1830-1835 https://doi.org/10.1002/eji.201040391

Kohl M, Wiese S, Warscheid B (2011): Cytoscape: software for visualization and analysis of biological networks. Methods Mol. Biol. **696,** 291-303 https://doi.org/10.1007/978-1-60761-987-1_18

Kumagai J, Kiuchi M, Kokubo K, Yagyu H, Nemoto M, Tsuji K, Nagahata K, Sasaki A, Hishiya T, Onoue M (2023): The USP7-STAT3-granzyme-Par-1 axis regulates allergic inflammation by promoting differentiation of IL-5-producing Th2 cells. Proc. Natl. Acad. Sci. USA **120,** e2302903120 https://doi.org/10.1073/pnas.2302903120

Li C, Li S, Liu J, Cai H, Liu G, Deng X, Chang W (2022): Escherichia coli O88 induces intestinal damage and inflammatory response through the oxidative phosphorylation and ribosome pathway in Pekin ducks. Front. Cell. Infect. Microbiol. **12,** 940847 https://doi.org/10.3389/fcimb.2022.940847

Lin L, Li T, Sun M, Liang Q, Ma Y, Wang F, Duan J, Sun Z (2021): Effect of particulate matter exposure on the prevalence of allergic rhinitis in children: a systematic review and meta-analysis. Chemosphere **268,** 128841 https://doi.org/10.1016/j.chemosphere.2020.128841

Martinvalet D, Zhu P, Lieberman J (2005): Granzyme A induces caspase-independent mitochondrial damage, a required first step for apoptosis. Immunity **22,** 355-370 https://doi.org/10.1016/j.immuni.2005.02.004

Moreno-Martinez L, Santiago L, de la Torre M, Calvo A, Pardo J, Osta RJIjoms (2022): Hemizygous granzyme A mice expressing the hSOD1G93A transgene show slightly extended lifespan. Int. J. Mol. Sci. **23,** 13554 https://doi.org/10.3390/ijms232113554

Nur Husna SM, Md Shukri N, Tuan Sharif SE, Tan HTT, Mohd Ashari NS, Wong KK (2022a): IL-4/IL-13 axis in allergic rhinitis: elevated serum cytokines levels and inverse association with tight junction molecules expression. Front. Mol. Biosci. **9,** 819772 https://doi.org/10.3389/fmolb.2022.819772

Nur Husna SM, Tan H-TT, Md Shukri N, Mohd Ashari NS, Wong KK (2022b): Allergic rhinitis: a clinical and pathophysiological overview. Front. Med. **9,** 874114

https://doi.org/10.3389/fmed.2022.874114
Pang K, Li G, Li M, Zhang L, Fu Q, Liu K, Zheng W, Wang Z, Zhong J, Lu L (2022): Prevalence and risk factors for allergic rhinitis in China: a systematic review and meta-analysis. Evid. Based Complement. Alternat. Med. **2022,** 7165627 https://doi.org/10.1155/2022/7165627
Park S, Griesenauer B, Jiang H, Adom D, Mehrpouya-Bahrami P, Chakravorty S, Kazemian M, Imam T, Srivastava R, Hayes TA (2020): Granzyme A-producing T helper cells are critical for acute graft-versus-host disease. JCI Insight **5,** e124465 https://doi.org/10.1172/jci.insight.124465
Qayum AA, Hayes T, Kaplan MH (2020): JAK-STAT signaling in asthma and allergic airway inflammation. In: JAK-STAT Signaling in Diseases. (Ed. Goswami R), pp. 49-68, CRC Press https://doi.org/10.1201/9781351042468-4
Ren M, Wang Y, Lin L, Li S, Ma Q (2022): α-linolenic acid screened by molecular docking attenuates inflammation by regulating Th1/Th2 imbalance in ovalbumin-induced mice of allergic rhinitis. Molecules **27,** 5893 https://doi.org/10.3390/molecules27185893
Ri H, Peiyan Z, Jianqi W, Yunteng Z, Gang L, Baoqing S (2019): Desmoglein 3 gene mediates epidermal growth factor/epidermal growth factor receptor signaling pathway involved in inflammatory response and immune function of anaphylactic rhinitis. Biomed. Pharmacother. **118,** 109214 https://doi.org/10.1016/j.biopha.2019.109214
Roskoski Jr R (2016): Janus kinase (JAK) inhibitors in the treatment of inflammatory and neoplastic diseases. Pharmacol. Res. **111,** 784-803 https://doi.org/10.1016/j.phrs.2016.07.038
Saito H, Matsumoto K, Denburg AE, Crawford L, Ellis R, Inman MD, Sehmi R, Takatsu K, Matthaei KI, Denburg JA (2002): Pathogenesis of murine experimental allergic rhinitis: a study of local and systemic consequences of IL-5 deficiency. J. Immunol. **168,** 3017-3023 https://doi.org/10.4049/jimmunol.168.6.3017
Schanoski AS, Le TT, Kaiserman D, Rowe C, Prow NA, Barboza DD, Santos CA, Zanotto PM, Magalhães KG, Aurelio L (2020): Granzyme A in chikungunya and other arboviral infections. Front. Immunol. **10,** 3083 https://doi.org/10.3389/fimmu.2019.03083
Shankar A, McAlees JW, Lewkowich IP (2022): Modulation of IL-4/IL-13 cytokine signaling in the context of allergic disease. J. Allergy Clin. Immunol. **150,** 266-276 https://doi.org/10.1016/j.jaci.2022.06.012
Shi Z, Jiang W, Wang M, Wang X, Li X, Chen X, Qiao L (2017): Inhibition of JAK/STAT pathway restrains TSLP-activated dendritic cells mediated inflammatory T helper type 2 cell response in allergic rhinitis. Mol. Cell. Biochem. **430,** 161-169 https://doi.org/10.1007/s11010-017-2963-7
Shimizu K, Yamasaki S, Sakurai M, Yumoto N, Ikeda M, Mishima-Tsumagari C, Kukimoto-Niino M, Watanabe T, Kawamura M, Shirouzu M (2019): Granzyme A stimulates pDCs to promote adaptive immunity via induction of type I IFN. Front. Immunol. **10,** 1450 https://doi.org/10.3389/fimmu.2019.01450
Subramanian A, Tamayo P, Mootha VK, Mukherjee S, Ebert BL, Gillette MA, Paulovich A, Pomeroy SL, Golub TR, Lander ES (2005): Gene set enrichment analysis: a knowledge-based approach for interpreting genome-wide expression profiles. Proc. Natl. Acad. Sci. USA **102,** 15545-15550 https://doi.org/10.1073/pnas.0506580102
Sun Y, Liu T, Bai W (2022): MAF bZIP transcription factor B (MAFB) protected against ovalbumin-induced allergic rhinitis via the alleviation of inflammation by restoring the T helper (Th) 1/Th2/Th17 imbalance and epithelial barrier dysfunction. J. Asthma Allergy **15,** 267-280 https://doi.org/10.2147/JAA.S335560
Torres DG, Paes J, da Costa AG, Malheiro A, Silva GV, Mourão LPdS, Tarragô AM (2022): JAK2 variant signaling: Genetic, hematologic and immune implication in chronic myeloproliferative neoplasms. Biomolecules **12,** 291 https://doi.org/10.3390/biom12020291
Voss AK, Strasser A (2020): The essentials of developmental apoptosis. F1000Res. **9,** 148 https://doi.org/10.12688/f1000research.21571.1
Wang W, Wang Q, Wan D, Sun Y, Wang L, Chen H, Liu C, Petersen RB, Li J, Xue W (2017): Histone HIST1H1C/H1. 2 regulates autophagy in the development of diabetic retinopathy. Autophagy **13,** 941-954 https://doi.org/10.1080/15548627.2017.1293768
Wei T, Simko V, Levy M, Xie Y, Jin Y, Zemla J (2017): Package ‚corrplot'. Statistician **56,** e24
Wilke CO (2018): ggridges: ridgeline plots in ‚ggplot2'. R package version 05. **1,** 483 https://doi.org/10.32614/CRAN.package.ggridges
Xue C, Yao Q, Gu X, Shi Q, Yuan X, Chu Q, Bao Z, Lu J, Li L (2023): Evolving cognition of the JAK-STAT signaling pathway: autoimmune disorders and cancer. Signal. Transduct. Target Ther. **8,** 204 https://doi.org/10.1038/s41392-023-01468-7
Yu X, Wang M, Zhao H, Cao Z (2021): Targeting a novel hsa_circ_0000520/miR-556-5p/NLRP3 pathway-mediated cell pyroptosis and inflammation attenuates ovalbumin (OVA)-induced allergic rhinitis (AR) in mice models. Inflamm. Res. **70,** 719-729 https://doi.org/10.1007/s00011-021-01472-z
Zak M, Hanan EJ, Lupardus P, Brown DG, Robinson C, Siu M, Lyssikatos JP, Romero FA, Zhao G, Kellar T (2019): Discovery of a class of highly potent Janus Kinase 1/2 (JAK1/2) inhibitors demonstrating effective cell-based blockade of IL-13 signaling. Bioorg. Med. Chem. Lett. **29,** 1522-1531 https://doi.org/10.1016/j.bmcl.2019.04.008
Zhang J-j, He X-c, Zhou M, Liu Q-d, Xu W-z, Yan Y-j, Ruan Y (2023): Xiao-qing-long-tang ameliorates OVA-induced allergic rhinitis by inhibiting ILC2s through the IL-33/ST2 and JAK/STAT pathways. Phytomedicine **119,** 155012 https://doi.org/10.1016/j.phymed.2023.155012
Zhang Y, Lan F, Zhang L (2022): Update on pathomechanisms and treatments in allergic rhinitis. Allergy **77,** 3309-3319 https://doi.org/10.1111/all.15454
Zhou Z, He H, Wang K, Shi X, Wang Y, Su Y, Wang Y, Li D, Liu W, Zhang Y (2020): Granzyme A from cytotoxic cleaves GSDMB to trigger pyroptosis in target cells. Science **368,** eaaz7548 https://doi.org/10.1126/science.aaz7548

Received: August 8, 2024
Final version accepted: November 5, 2024

doi: 10.4149/gpb_2024045

Supplementary Material

GZMA silencing inhibits JAK2/STAT1 pathway and improves allergic rhinitis

Lin Li[1], Yuhao Zhang[1], Jingyuan Wang[1], Lixia Zhang[1], Ying Gao[1], Xiaolin Ji[1], Tian Wang[1] and Fei Zhao[1]

[1] *Department of Otolaryngology Head and Neck Surgery, Shanxi Bethune Hospital, Shanxi Academy of Medical Sciences, Third Hospital of Shanxi Medical University, Tongji Shanxi Hospital, Taiyuan, Shanxi, China*

Supplementary Figure

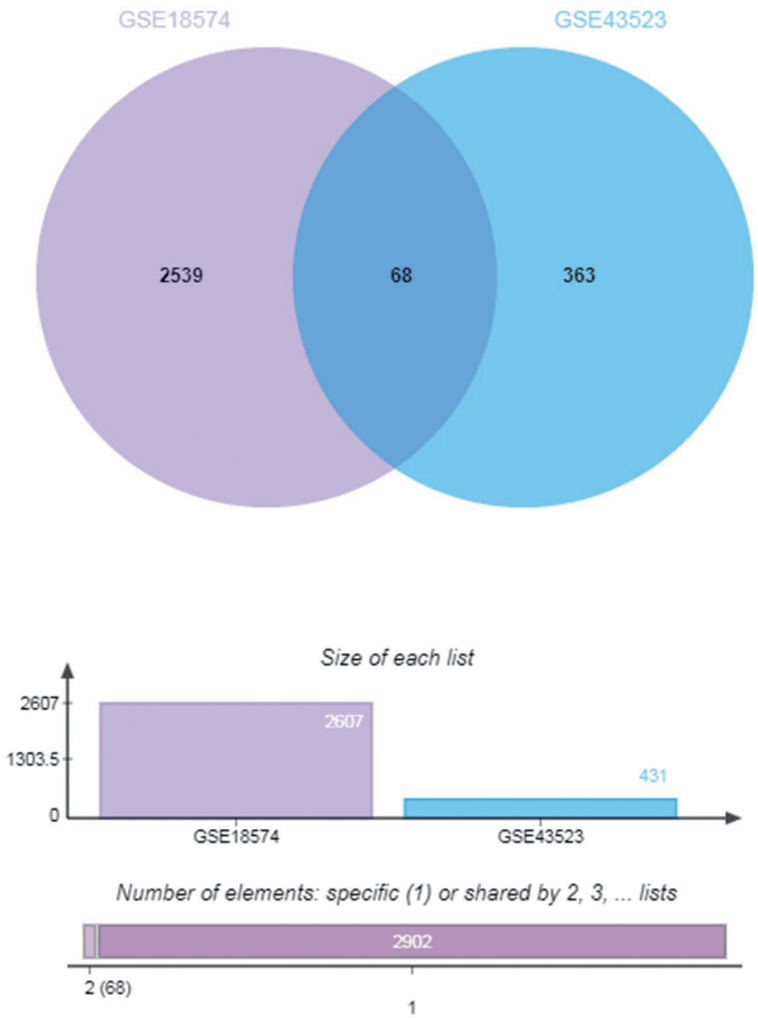

Figure S1. Venn diagram showing 68 co-DEGs at the intersection of GSE18574 and GSE43523 datasets

Supplementary Tables

Table S1. The primer sequences for qRT-PCR

Name	Sequences
si-GZMA-1-Sense	GAUAUUGACUGUUAAGAAAGC
si-GZMA-1-Antisense	UUUCUUAACAGUCAAUAUCUG
si-GZMA-2-Sense	GGUUGUUCCUCACUCAAGACC
si-GZMA-2-Antisense	UCUUGAGUGAGGAACAACCGU
si-NC-Sense	UUCUCCGAACGUGUCACGUTT
si-NC-Antisense	ACGUGACACGUUCGGAGAATT
oe-GZMA-F	CGCGGATCCATGAGGAACGCCTCTG
oe-GZMA-R	CCGCTCGAGCACAGAACCTTCATA

Table S2. The top 15 upregulated and top 15 downregulated genes in GSE18574 dataset

Name	**Description**	**log2FC**	***p* value**	**up/down**
IL17RB	interleukin 17 receptor B	8.93	1.23E−04	up
TOP2A	topoisomerase (DNA) II alpha	7.20	4.64E−04	up
KIF15	kinesin family member 15	6.63	1.26E−02	up
LAG3	lymphocyte activating 3	6.50	2.56E−04	up
ZBTB32	zinc finger and BTB domain containing 32	6.39	1.91E−05	up
GZMB	granzyme B	5.98	3.22E−05	up
TYMS	thymidylate synthetase	5.69	2.64E−05	up
PHC3	polyhomeotic homolog 3	5.62	4.18E−03	up
POU2AF1	POU class 2 associating factor 1	5.52	3.06E−02	up
ASB2	ankyrin repeat and SOCS box containing 2	5.50	5.88E−04	up
ASPM	abnormal spindle microtubule assembly	5.38	1.98E−04	up
GINS2	GINS complex subunit 2	5.33	2.27E−05	up
DUSP4	dual specificity phosphatase 4	5.32	3.08E−06	up
CCL20	C−C motif chemokine ligand 20	5.30	3.55E−03	up
UHRF1	ubiquitin like with PHD and ring finger domains 1	5.27	1.69E−04	up
LTC4S	leukotriene C4 synthase	−4.49	1.62E−04	down
RDH16	retinol dehydrogenase 16 (all-trans)	−4.67	3.90E−02	down
P2RY6	pyrimidinergic receptor P2Y6	−4.74	3.15E−03	down
FUCA1	fucosidase, alpha-L-1, tissue	−4.77	2.67E−05	down
TMIGD3	transmembrane and immunoglobulin domain containing 3	−4.98	3.98E−03	down
C1QC	complement C1q C chain	−5.08	4.18E−04	down
GFRA2	GDNF family receptor alpha 2	−5.39	4.36E−02	down
LILRB5	leukocyte immunoglobulin like receptor B5	−5.46	7.42E−03	down
FCN1	ficolin 1	−5.54	2.81E−04	down
KRT72	keratin 72	−5.62	1.10E−02	down
SERPINB2	serpin family B member 2	−5.76	5.05E−05	down
CLEC10A	C-type lectin domain family 10 member A	−6.03	5.95E−04	down
MPEG1	macrophage expressed 1	−6.21	6.90E−05	down
STAB1	stabilin 1	−7.45	2.59E−04	down
CCL2	C−C motif chemokine ligand 2	−8.64	4.04E−05	down

Table S3. The top 15 upregulated and top 15 downregulated genes in GSE43523 dataset

Name	Description	log2FC	*p* value	up/down
CST1	cystatin SN	6.01	8.54E−04	up
ITLN1	intelectin 1	4.08	4.14E−03	up
CD69	CD69 molecule	2.62	1.00E−02	up
CLC	Charcot-Leyden crystal galectin	2.57	1.13E−03	up
CDH26	cadherin 26	2.39	5.48E−04	up
TFF3	trefoil factor 3	2.19	1.08E−02	up
CCL26	C−C motif chemokine ligand 26	2.10	8.94E−03	up
MUC2	mucin 2, oligomeric mucus/gel-forming	2.06	3.81E−02	up
GZMB	granzyme B	1.94	3.75E−02	up
LRRC23	leucine rich repeat containing 23	1.87	4.73E−02	up
CD52	CD52 molecule	1.77	1.34E−02	up
HDC	histidine decarboxylase	1.75	6.57E−03	up
FABP6	fatty acid binding protein 6	1.69	1.37E−02	up
CACNG6	calcium voltage-gated channel auxiliary subunit gamma 6	1.69	4.52E−02	up
RGS1	regulator of G-protein signaling 1	1.63	4.17E−02	up
PPFIA1	PTPRF interacting protein alpha 1	−1.24	4.21E−03	down
SPATA13	spermatogenesis associated 13	−1.24	3.28E−02	down
SYT7	synaptotagmin 7	−1.25	2.02E−03	down
XDH	xanthine dehydrogenase	−1.25	3.24E−02	down
AKR1B1	aldo-keto reductase family 1 member B	−1.26	1.48E−04	down
ST3GAL5	ST3 beta−galactoside alpha-2,3-sialyltransferase 5	−1.28	1.17E−04	down
DUOX2	dual oxidase 2	−1.28	2.55E−02	down
AKR1B10	aldo-keto reductase family 1 member B10	−1.33	3.53E−02	down
TGFBRAP1	transforming growth factor beta receptor associated protein 1	−1.38	1.44E−02	down
OTX1	orthodenticle homeobox 1	−1.51	7.66E−03	down
RORA	RAR related orphan receptor A	−1.55	6.54E−03	down
SERPINE2	serpin family E member 2	−1.60	1.63E−02	down
PDE5A	phosphodiesterase 5A	−1.64	1.88E−04	down
SERPINB7	serpin family B member 7	−1.74	1.85E−02	down
ANKRD36B	ankyrin repeat domain 36B	−2.45	1.05E−03	down